

Microcanonical rates, gap times,
and phase space dividing surfaces

Gregory S. Ezra*

Department of Chemistry and Chemical Biology

Baker Laboratory

Cornell University

Ithaca, NY 14853

USA

Holger Waalkens[†]

University of Groningen

Institute of Mathematics and Computing Science

P.O. Box 407

9700 AK Groningen

The Netherlands

Stephen Wiggins[‡]

School of Mathematics

University of Bristol

Bristol BS8 1TW

United Kingdom

(Dated: October 25, 2021)

Abstract

The general approach to classical unimolecular reaction rates due to Thiele is revisited in light of recent advances in the phase space formulation of transition state theory for multidimensional systems. Key concepts such as the phase space dividing surface separating reactants from products, the average gap time, and the volume of phase space associated with reactive trajectories, are both rigorously defined and readily computed within the phase space approach. We analyze in detail the gap time distribution and associated reactant lifetime distribution for the isomerization reaction $\text{HCN} \rightleftharpoons \text{CNH}$, previously studied using the methods of phase space transition state theory. Both algebraic (power law) and exponential decay regimes have been identified. Statistical estimates of the isomerization rate are compared with the numerically determined decay rate. Correcting the RRKM estimate to account for the measure of the reactant phase space region occupied by trapped trajectories results in a drastic overestimate of the isomerization rate. Compensating but as yet poorly understood trapping mechanisms in the reactant region serve to slow the escape rate sufficiently that the uncorrected RRKM estimate turns out to be reasonably accurate, at least at the particular energy studied. Examination of the decay properties of subsensembles of trajectories that exit the HCN well through either of 2 available symmetry related product channels shows that the complete trajectory ensemble effectively attains the full symmetry of the system phase space on a short timescale $t \lesssim 0.5$ ps, after which the product branching ratio is 1:1, the “statistical” value. At intermediate times, this statistical product ratio is accompanied by nonexponential (nonstatistical) decay. We point out close parallels between the dynamical behavior inferred from the gap time distribution for HCN and nonstatistical behavior recently identified in reactions of some organic molecules.

PACS numbers: 05.45.-a, 82.20.-w, 82.20.Db, 82.30.Qt

I. INTRODUCTION

The theory of unimolecular reaction rates, both for dissociative and isomerization processes, has been of great interest for nearly a century¹. Following the original formulation of the statistical RRK and RRKM approaches to calculation of reaction rates^{2,3,4,5,6}, there has been a vast amount of activity, some of which has been described in several generations of textbooks^{7,8,9,10,11,12,13,14,15,16,17,18,19,20,21,22,23,24}. For concise overviews of the historical development of unimolecular rate theory, see Forst²³, Chapter 1, also ref. 25.

To provide the context for the discussion in the present paper, we highlight some important and relevant contributions to the subject. (The selection of works cited is necessarily quite limited.) The development of Slater’s “new” dynamical approach to classical unimolecular dissociation rates^{9,26} was followed by Thiele’s general formulation of the problem, which emphasized the dynamical significance of the distribution of gap times (see below)²⁷. As we show below, Thiele’s work has proved to be remarkably prescient in terms of its identification of the appropriate phase space structures involved in unimolecular reaction dynamics. Following Thiele’s work, a large number of computational (trajectory) investigations of lifetime/gap time distributions have been undertaken (see, for example, results discussed in^{10,22,28}). Dumont and Brumer^{29,30} and Dumont^{31,32,33,34} have analysed unimolecular reaction rates in terms of the gap time distribution, while related work has been done on the so-called classical spectral theorem^{35,36}.

A fundamental assumption of the statistical theory of (classical) unimolecular decay is that intramolecular vibrational energy distribution (IVR) occurs on a timescale much faster than that for reaction^{14,22}. Renewed interest in the problem therefore naturally stemmed from investigations of the properties of molecular vibrational dynamics, modelled as nonlinearly coupled anharmonic oscillators, in light of the KAM theorem and the apparent existence of a threshold energy for onset of global chaos^{37,38,39,40}. The central role of deterministic chaos itself in determining the validity of statistical approaches to reaction rates, as well as possible quantum manifestations of classical nonintegrable behavior⁴¹, has received much attention⁴⁰, most recently in the context of quantum control^{42,43}. The possibility of mode-specific chemistry also stimulated much work on the relation between intramolecular dynamics and non-statistical reaction dynamics⁴⁴. Several examples of non-RRKM effects in thermal reactions of medium-sized organic molecules have been found in recent

years^{45,46,47,48}, while a detailed discussion of possible non-RRKM effects in one particular reaction, the unimolecular dissociation of H_3^+ , has been given⁴⁹.

Advances in the classical theory of chemical reaction rates have been closely linked to improvements in our understanding of the phase space structure of Hamiltonian systems^{50,51,52,53}. Both conceptually and in practice it is important to distinguish between systems with 2 degrees of freedom (DoF) and multimode ($N \geq 3$ DoF) systems.

For 2 DoF systems described by standard kinetic plus potential Hamiltonians, periodic orbit dividing surfaces (PODS; that is, dividing surfaces in configuration space obtained by projection of a periodic orbit from phase space) were shown to have the property of minimal flux (as a consequence of the principle of stationary action) and to be (locally) surfaces of no return (the velocity vector is nowhere tangent to the configuration space projection of the periodic orbit)^{54,55,56}. In this case the PODS therefore provide a rigorous realization of the concept of the transition state^{57,58}. (PODS have also been defined for 2 DoF systems lacking time-reversal symmetry⁵⁹.) Correlations between features of the classical phase space structure and the behavior of the computed reactive flux^{60,61} were explored relatively early on for 2 DoF systems by DeLeon and Berne^{62,63}. Important theoretical advances were subsequently made relating non-statistical behavior to molecular phase space structure⁶⁴, in particular the existence of intramolecular bottlenecks to energy transfer^{65,66,67}, broken separatrices^{68,69,70}, and reactive islands and cylinders^{71,72,73,74,75,76,77}.

The multimode case remains less thoroughly explored and understood. Methods for defining approximate intramolecular bottlenecks and reactive dividing surfaces have been devised^{78,79,80,81,82,83,84}. Although the Arnold web of resonances provides a useful framework for mapping and analyzing evolution of phase points in near-integrable multimode systems^{51,85}, so-called “Arnold diffusion”^{51,86} has become a convenient but often ill-defined catchall term employed to describe a variety of possibly distinct phase space transport mechanisms in $N \geq 3$ DoF systems⁸⁷. The possible role of “Arnold diffusion” in multimode molecular systems has been studied in IVR^{85,88,89,90,91} and in isomerization^{92,93}. Local random matrix theories have served as the foundation for quantum theoretical treatments of isomerization reactions in large molecules^{94,95,96,97,98}, while attention has also been given to related scaling approaches^{99,100,101} and to fractional kinetics^{102,103,104}.

An important advance was the realization that normally hyperbolic invariant manifolds (NHIMs^{105,106}) provide a natural and theoretically well-founded generalization of PODS to

the $N \geq 3$ DoF case (cf. ref. 107). The stable and unstable manifolds associated with NHIMs define codimension-one dividing surfaces¹⁰⁸ on the constant energy manifold^{105,106}, and so are possible candidates for reactive separatrices, while the NHIMs themselves define phase space transition states^{109,110}. Some early attempts were made to compute and visualize such manifolds in a 3 DoF system describing surface diffusion of atoms¹¹¹ and for a 4D symplectic mapping modelling the dissociation of a van der Waals complex^{112,113}.

As discussed in more detail below, based on the notion of the NHIM and on the development of efficient algorithms for computing normal forms at saddles, there has been significant recent progress in the development and implementation of phase space transition state theory^{105,109,110,114,115,116,117,118,119,120} (see also^{93,121,122,123,124,125,126,127,128}).

In the present paper we consider the problem of defining and evaluating theoretical unimolecular reaction rates in light of the penetrating analyses of Thiele²⁷, Dumont and Brumer²⁹, and DeLeon and Berne^{62,63}, the classical spectral theorem^{35,36}, and the recent developments in phase space transition state theory^{109,110,114,115,116,117,118,119,120} mentioned above. The particular reaction chosen for study is the isomerization $\text{HCN} \rightleftharpoons \text{CNH}$ ^{116,117,129,130,131,132,133,134,135,136,137}, for which several relevant theoretical quantities have recently been computed for a (classical) model of the HCN molecule at fixed energy^{116,117}.

We are concerned with the rate of reaction, at fixed energy, for a system described by a time-independent, n degree-of-freedom (DOF) classical Hamiltonian. One measure of the rate at which trajectories leave a region of the energy surface is given by the (magnitude of the) flux of trajectories leaving that region (units of energy surface volume/time) divided by the energy surface volume of initial conditions in that region *corresponding to trajectories that will eventually leave the region*. This rate is just the inverse of the mean passage or gap time^{27,29}. Hence, to compute this rate at fixed energy one must first (1) define the region of reactants, then (2) compute the flux of trajectories exiting this region and, finally, (3) compute the volume of the energy surface corresponding to initial conditions of trajectories that leave the reactant region.

The importance of the gap time distribution was emphasized by Thiele²⁷, who explicitly invoked the concept of a phase space dividing surface separating reactants and products^{138,139}. While the use of dividing surfaces (transition states) defined in configuration space is quite familiar in the field of reaction rate theory^{58,140}, carrying out these steps in phase space, as opposed to configuration space, remains less familiar in practice^{64,84}. In the

present paper we show how the expression for the microcanonical rate of reaction described above can be evaluated using the phase space approach to reaction dynamics developed in a recent series of papers^{109,110,114,115,116,117,118,119,120}. Moreover, we analyze in detail the properties of the gap time distribution previously obtained for HCN isomerization using the phase space reaction rate theory¹¹⁷.

The structure of the paper is as follows: in Section II we outline an approach to the classical theory of unimolecular reaction rates based upon the general formulation of Thiele²⁷. We demonstrate that various dynamical quantities related to the unimolecular reaction rate defined within Thiele’s approach can be rigorously defined and computed within the recently developed theoretical framework for phase space transition state theory^{109,110,114,115,116,117,118,119,120}. Special emphasis is placed on the properties of the gap time distribution, and the relation between the inverse gap time and the rate of reaction. In Section III we consider the dynamics of the HCN isomerization reaction. We analyze previously computed classical trajectory results^{116,117} in light of the discussion given in Section II. Both gap time and reactant lifetime distributions are analyzed, and distinct temporal regimes identified, with power law (algebraic) decay seen at intermediate times and exponential decay at long times. Moreover, we find a statistical (1:1) product ratio for both algebraic and exponential decay regimes. Comparisons are made between computed values of the decay rate and statistical estimates of the isomerization rate. Our results show that analysis of gap time distributions computed using phase space dividing surfaces having minimal flux and no-recrossing properties yields a great deal of information about the system dynamics. Section IV concludes.

II. GENERAL APPROACH TO UNIMOLECULAR REACTION RATES

In this section we present a general formulation of unimolecular reaction rates based upon that originally given by Thiele²⁷. In their general form the rate expressions derived by Thiele explicitly invoke the existence of a *phase space* dividing surface separating reactants and products; such surfaces, although discussed by Wigner¹³⁸ at the inception of the theory of chemical reaction rates (see also^{139,140}), have only recently become amenable to direct computation via the use of normal form approaches^{109,110,114,115,116,117,118,119,120,121,122,123}

A. Phase space dividing surfaces: definition and properties

We are concerned with the rate of unimolecular reactions, either dissociation or isomerization, at fixed energy, for a system described by a time-independent, n degree-of-freedom (DOF) classical Hamiltonian. Points in the $2n$ -dimensional system phase space $\mathcal{M} = \mathbb{R}^{2n}$ are denoted $\mathbf{x} \in \mathcal{M}$. The system Hamiltonian is $H(\mathbf{x})$, and the $(2n - 1)$ dimensional energy shell at energy E , $H(\mathbf{x}) = E$, is denoted $\Sigma_E \subset \mathcal{M}$. The corresponding microcanonical phase space density is $\delta(E - H(\mathbf{x}))$, and the associated density of states for the complete energy shell at energy E is

$$\rho(E) = \int_{\mathcal{M}} d\mathbf{x} \delta(E - H(\mathbf{x})). \quad (2.1)$$

The first step in the analysis is to define the region of the energy surface corresponding to the reactant of interest. For complex systems there may be many such regions of interest¹⁴¹, but for the moment we focus on only one such region, and the rate at which trajectories leave that particular region. We treat either unimolecular dissociations or isomerizations in which molecules are removed from consideration immediately after passing from the reactant region of phase space, and are not therefore directly concerned here with reactive flux correlation functions or associated relaxation kinetics^{31,32,60,61,70}.

A standard approach to defining the reactant region is to consider the potential energy function—a configuration space based approach¹⁴¹. In the simplest case the reactant region is associated with a single local minimum, and trajectories exit/enter the reactant region by passing over energetically accessible saddle points of the potential. Although there could be several saddles controlling rates of exit from the potential well, as mentioned we will only consider the case of a single saddle. We comment on the case of multiple saddles below.

However, dynamics occurs in phase space (i.e., on the energy surface $\Sigma_E \subset \mathcal{M}$ for the situation we are considering) while the picture described above is concerned with the projection of trajectories from phase space to configuration space. For multidimensional systems such as polyatomic molecules ($N \geq 3$ DoF), it is in general no longer possible to define or compute a dividing surface with desirable dynamical attributes such as the nonrecrossing property by working in configuration space alone, and a phase space perspective is necessary^{109,110,114,115,116,117,118,119,120,121,122,123}.

While the phase space approach to reaction dynamics reviewed briefly below does not give a complete solution to the problem (questions of transition state bifurcations and non-integrability remain to be addressed, for example), it does provide an important component, which, when coupled with knowledge of certain properties of the system Hamiltonian function, does provide the necessary information to identify the reactant region in some situations of interest. Saddle points of the potential energy surface still play a role – in particular, rank one saddles. For Hamiltonian functions that are the sum of the kinetic energy and the potential energy a rank one saddle point of the potential energy function is manifested as an equilibrium point of saddle type for the $2n$ dimensional Hamilton’s equations¹⁰⁶. More precisely, it is an equilibrium point of saddle-center-...-center stability type, meaning that the $2n \times 2n$ matrix associated with the linearization of Hamilton’s equations about this equilibrium point has $2n$ eigenvalues of the form $\pm\lambda, \pm i\omega_k, k = 2, \dots, n$ ($\lambda, \omega_k > 0$). The significance of saddle points of this type for Hamilton’s equations is that, for a range of energies above that of the saddle (we explicitly discuss the range of energies later on), the energy surfaces have the *bottleneck property* in a phase space neighborhood near the saddle, i.e. the $2n - 1$ dimensional energy surface *locally* has the geometrical structure of the product of a $2n - 2$ dimensional sphere and an interval, $S^{2n-2} \times I$. The bottleneck property is significant because in the vicinity of the bottleneck we are able to construct a dividing surface, $DS(E)$, (where ‘ E ’ denotes the energy dependence) with very desirable properties. For each energy in this range above the saddle $DS(E)$ locally “disconnects” the energy surface into two, disjoint pieces with the consequence that the only way to pass from one piece of the energy surface to the other is to cross $DS(E)$. The dividing surface has the geometrical structure of a $2n - 2$ dimensional sphere, S^{2n-2} , which is divided into two $2n - 2$ dimensional hemispheres, denoted $DS_{\text{in}}(E)$ and $DS_{\text{out}}(E)$ that are joined at an equator, which is a $2n - 3$ dimensional sphere, S^{2n-3} . The hemisphere $DS_{\text{in}}(E)$ corresponds to initial conditions of

trajectories that enter the reaction region while $\text{DS}_{\text{out}}(E)$ corresponds to initial conditions of trajectories that exit the reaction region, both by passing through the bottleneck in the energy surface. The equator S^{2n-3} is an invariant manifold of saddle stability type, a so-called *normally hyperbolic invariant manifold* (NHIM)¹⁰⁶. The NHIM acts as the “anchor” for this entire construction and is of great physical significance: it is the actual “saddle” in phase space identified as the “activated complex” of reaction rate dynamics^{58,107,120}). Our focus here is on microcanonical rates, and it has been shown that $\text{DS}_{\text{in}}(E)$ and $\text{DS}_{\text{out}}(E)$ have the essential *no-recrossing property* and that the flux across them is minimal¹¹⁵. We denote the directional flux across these hemispheres by $\phi_{\text{in}}(E)$ and $\phi_{\text{out}}(E)$, respectively, and note that $\phi_{\text{in}}(E) + \phi_{\text{out}}(E) = 0$. For our purposes we only need the magnitude of the flux, and so set $|\phi_{\text{in}}(E)| = |\phi_{\text{out}}(E)| \equiv \phi(E)$. Most significantly, the hemisphere $\text{DS}_{\text{in}}(E)$ is the correct surface across which to compute the “exact” flux into the reaction region.

B. Phase space volumes and gap times

The disjoint regions of phase space corresponding to species A (reactant) and B (product) will be denoted \mathcal{M}_A and \mathcal{M}_B , respectively¹⁴². We assume that all coordinates and momenta are bounded on the reactant energy shell $\Sigma_E \cap \mathcal{M}_A$, and that it is possible to define a boundary (dividing surface) DS in phase space separating species A and B. As discussed above, the DS can be rigorously defined to be locally a surface of no return (transition state). The microcanonical density of states for reactant species A is

$$\rho_A(E) = \int_{\mathcal{M}_A} d\mathbf{x} \, \delta(E - H(\mathbf{x})) \quad (2.2)$$

with a corresponding expression for the density of states $\rho_B(E)$ for product B for the case of compact product energy shell \mathcal{M}_B .

Provided that the flow is everywhere transverse to $\text{DS}_{\text{in, out}}(E)$, those phase points in the reactant region \mathcal{M}_A that lie on crossing trajectories^{62,63} (i.e., that will react, and so are “interesting” in Slater’s terminology⁹) can be specified uniquely by coordinates $(\bar{\mathbf{q}}, \bar{\mathbf{p}}, \psi)$, where $(\bar{\mathbf{q}}, \bar{\mathbf{p}}) \in \text{DS}_{\text{in}}(E)$ is a point on $\text{DS}_{\text{in}}(E)$, the incoming half of the DS, specified by $2(n-1)$ coordinates $(\bar{\mathbf{q}}, \bar{\mathbf{p}})$, and ψ is a time variable. (Dividing surfaces constructed by the normal form algorithm are guaranteed to be transverse to the vector field, except at the NHIM, where the vector field is tangent^{109,110}.) The point $\mathbf{x}(\bar{\mathbf{q}}, \bar{\mathbf{p}}, \psi)$ is reached by

propagating the initial condition $(\bar{\mathbf{q}}, \bar{\mathbf{p}}) \in \text{DS}_{\text{in}}(E)$ forward for time ψ (see Figure 1). As all initial conditions on $\text{DS}_{\text{in}}(E)$ (apart from a set of trajectories of measure zero lying on stable manifolds) will leave the reactant region in finite time by crossing $\text{DS}_{\text{out}}(E)$, for each $(\bar{\mathbf{q}}, \bar{\mathbf{p}}) \in \text{DS}_{\text{in}}(E)$ we can define the *gap time* $s = s(\bar{\mathbf{q}}, \bar{\mathbf{p}})$, which is the time it takes for the incoming trajectory to traverse the reactant region. That is, $\mathbf{x}(\bar{\mathbf{q}}, \bar{\mathbf{p}}, \psi = s(\bar{\mathbf{q}}, \bar{\mathbf{p}})) \in \text{DS}_{\text{out}}(E)$. For the phase point $\mathbf{x}(\bar{\mathbf{q}}, \bar{\mathbf{p}}, \psi)$, we therefore have $0 \leq \psi \leq s(\bar{\mathbf{q}}, \bar{\mathbf{p}})$.

The coordinate transformation $\mathbf{x} \rightarrow (E, \psi, \bar{\mathbf{q}}, \bar{\mathbf{p}})$ is canonical^{27,143,144,145}, so that the phase space volume element is

$$d^{2n}\mathbf{x} = dE d\psi d\sigma \quad (2.3)$$

with $d\sigma \equiv d^{n-1}\bar{\mathbf{q}} d^{n-1}\bar{\mathbf{p}}$ an element of $2n - 2$ dimensional area on the DS.

As defined above, the magnitude $\phi(E)$ of the flux through dividing surface $\text{DS}(E)$ at energy E is given by

$$\phi(E) = \left| \int_{\text{DS}_{\text{in}}(E)} d\sigma \right|, \quad (2.4)$$

where the element of area $d\sigma$ is precisely the restriction to DS of the appropriate flux $(2n - 2)$ -form $\omega^{(n-1)}/(n - 1)!$ corresponding to the Hamiltonian vector field associated with $H(\mathbf{x})$ ^{111,115,146,147}. The reactant phase space volume occupied by points initiated on the dividing surface DS_{in} with energies between E and $E + dE$ is therefore^{27,35,36,117,118,144,145}

$$dE \int_{\text{DS}_{\text{in}}(E)} d\sigma \int_0^s d\psi = dE \int_{\text{DS}_{\text{in}}(E)} d\sigma s \quad (2.5a)$$

$$= dE \phi(E) \bar{s} \quad (2.5b)$$

where the *mean gap time* \bar{s} is defined as

$$\bar{s} = \frac{1}{\phi(E)} \int_{\text{DS}_{\text{in}}(E)} d\sigma s \quad (2.6)$$

and is a function of energy E . The reactant density of states $\rho_A^{\text{C}}(E)$ associated with crossing trajectories only (those trajectories that enter and exit the reactant region⁶³; see below) is then

$$\rho_A^{\text{C}}(E) = \phi(E) \bar{s} \quad (2.7)$$

where the superscript C indicates the restriction to crossing trajectories. The result (2.7) is essentially the content of the so-called classical spectral theorem^{35,36,117,118,144,145}.

If *all* points in the reactant region of phase space eventually react (that is, all points lie on crossing trajectories^{62,63}) then $\rho_A^{\text{C}}(E) = \rho_A(E)$, the full reactant phase space density of

states. Apart from a set of measure zero, all phase points $\mathbf{x} \in \mathcal{M}_A$ can be classified as either trapped (T) or crossing (C)⁶³. (Further discussion of this division of the reactant phase space in terms of the Poincaré recurrence theorem is given in Appendix A.) A phase point in the trapped region \mathcal{M}_A^T never crosses the DS, so that the associated trajectory does not contribute to the reactive flux. Phase points in the crossing region \mathcal{M}_A^C do however eventually cross the dividing surface, and so lie on trajectories that contribute to the reactive flux. In general, however, as a consequence of the existence of trapped trajectories (either trajectories on invariant *trapped* n -tori^{62,63} or trajectories asymptotic to other invariant objects of zero measure), we have the inequality^{27,63}

$$\rho_A^C(E) \leq \rho_A(E). \quad (2.8)$$

If $\rho_A^C(E) < \rho_A(E)$, then it is in principle necessary to introduce corrections to statistical estimates of reaction rates^{49,63,70,148}. Numerical results for $\rho^C(E)$ and $\rho(E)$ for the HCN molecule are discussed below^{116,117}.

C. Gap time and reactant lifetime distributions

Of central interest is the *gap time distribution*, $\mathcal{P}(s; E)$: the probability that a phase point on $\text{DS}_{\text{in}}(E)$ at energy E has a gap time between s and $s + ds$ is equal to $\mathcal{P}(s; E)ds$. An important idealized gap distribution is the random, exponential distribution

$$\mathcal{P}(s; E) = \mathbb{k}(E) e^{-\mathbb{k}(E)s} \quad (2.9)$$

characterized by a single decay constant \mathbb{k} (where \mathbb{k} depends on energy E), with corresponding mean gap time $\bar{s} = \mathbb{k}^{-1}$.

The lifetime (time to cross the dividing surface $\text{DS}_{\text{out}}(E)$) of phase point $\mathbf{x}(\bar{\mathbf{q}}, \bar{\mathbf{p}}, \psi)$ is $t = s(\bar{\mathbf{q}}, \bar{\mathbf{p}}) - \psi$ (cf. Fig. 1b). The volume of reactant phase space occupied by trajectories having lifetimes $t \geq t'$ at energy E is then

$$\text{Vol}(t \geq t'; E) = \phi(E) \int_{t'}^{+\infty} ds (s - t') \mathcal{P}(s; E) \quad (2.10)$$

so that the corresponding probability of an interesting phase point in the reactant region having a lifetime $t \geq t'$ is obtained by dividing this volume by the total volume occupied by points on crossing trajectories, $\phi(E)\bar{s}$,

$$\text{Prob}(t \geq t'; E) = \frac{1}{\bar{s}} \int_{t'}^{+\infty} ds \mathcal{P}(s; E)(s - t'). \quad (2.11)$$

The corresponding reactant *lifetime distribution function* $\mathbb{P}(t; E)$ at energy E is therefore

$$\mathbb{P}(t; E) = -\frac{d}{dt'} \text{Prob}(t \geq t'; E) \Big|_{t'=t} \quad (2.12a)$$

$$= \frac{1}{s} \int_t^{+\infty} ds \mathcal{P}(s; E) \quad (2.12b)$$

where the fraction of interesting (reactive) phase points having lifetimes between t and $t+dt$ is $\mathbb{P}(t; E)dt$. It is straightforward to verify that the lifetime distribution (2.12) is normalized. Note that an exponential gap distribution (2.9) implies that the reactant lifetime distribution $\mathbb{P}(t; E)$ is also exponential; both gap and lifetime distributions for realistic molecular potentials have been of great interest since the earliest days of trajectory simulations of unimolecular decay^{10,28}.

We emphasize that the rigorous relation (2.12) between the gap time distribution and the reactant lifetime distribution follows quite straightforwardly from our continuous time formulation of the problem using the canonical transformation of phase space variables eq. (2.3) and the properties of the dividing surfaces DS (cf. ref. 29).

A concise derivation of the delay differential equation for the Delayed Lifetime Gap Model²⁹ is presented in Appendix B.

D. Reaction rates

We start with the (classical) expression for the rate $k(T)$ of a collisionally activated unimolecular process at temperature T derived by Thiele^{9,26,27}. Using the notation established above, the rate coefficient $k(T)$ is

$$k(T) = \frac{1}{Z_A} \int_{E_0}^{+\infty} dE e^{-\beta E} \int_{\text{DS}_{\text{in}}(E)} d\sigma [1 - e^{-\omega s}] \quad (2.13a)$$

$$= \frac{1}{Z_A} \int_{E_0}^{+\infty} dE e^{-\beta E} \phi(E) [1 - \overline{e^{-\omega s}}]. \quad (2.13b)$$

Here, $Z_A(T)$ is the reactant partition function

$$Z_A = \int dE e^{-\beta E} \rho_A(E), \quad (2.14)$$

$\beta = 1/k_B T$, ω is the effective collision rate per molecule, E_0 is the threshold energy for reaction, and the overline in eq. (2.13b) denotes an average over the dividing surface $\text{DS}_{\text{in}}(E)$. The physical interpretation of expression (2.13) is that the thermal reaction rate $k(T)$ is given

by the average of the equilibrium activation rate times the probability that an activated phase point will react (that is, cross the dividing surface DS_{out}) before it suffers a (strong) deactivating collision.

We note that the rate expression (2.13) makes sense even though for larger energies E the dividing surface $\text{DS}_{\text{in}}(E)$ with desired dynamical properties might no longer exist, as the contribution from high energies is damped away by the exponential Boltzmann factor. (Thiele²⁷ assumed the existence of a suitable dividing surface for all energies E .)

The limiting expressions for $k(T)$ obtained at high and low pressures are of interest. At high pressures ($\omega \rightarrow \infty$) we have

$$k_{\infty}(T) \equiv \lim_{\omega \rightarrow \infty} k(T) = \frac{1}{Z_A} \int_{E_0}^{+\infty} dE e^{-\beta E} \int_{\text{DS}_{\text{in}}(E)} d\sigma \quad (2.15a)$$

$$= \frac{1}{Z_A} \int_{E_0}^{+\infty} dE e^{-\beta E} \phi(E) \quad (2.15b)$$

$$= \frac{1}{Z_A} \int_{E_0}^{+\infty} dE \rho_A(E) e^{-\beta E} k_f^{\text{RRKM}}(E) \quad (2.15c)$$

where the quantity

$$k_f^{\text{RRKM}}(E) \equiv \frac{\phi(E)}{\rho_A(E)} \quad (2.16)$$

is the statistical (RRKM) microcanonical rate for the forward reaction ($A \rightarrow B$) at energy E , the ratio of the magnitude of the flux $\phi(E)$ through $\text{DS}_{\text{in}}(E)$ to the total reactant density of states^{14,15}. The rate $k_{\infty}(T)$ is then the canonical average of the microcanonical statistical rate $k_f^{\text{RRKM}}(E)$. (The collision rate ω should not be so large that trajectories of systems crossing the dividing surface are significantly perturbed by collisions.)

Clearly, if $\rho_A(E) = \rho_A^C(E)$, then

$$k_f^{\text{RRKM}}(E) = \frac{1}{\bar{s}} \quad (2.17)$$

the inverse mean gap time. In general, the inverse of the mean gap time is

$$\frac{1}{\bar{s}} = \frac{\phi(E)}{\rho_A^C} \equiv k_{f,C}^{\text{RRKM}} \quad (2.18a)$$

$$= k_f^{\text{RRKM}} \left[\frac{\rho_A(E)}{\rho_A^C(E)} \right] \quad (2.18b)$$

$$\geq k_f^{\text{RRKM}}. \quad (2.18c)$$

The rate $k_{f,C}^{\text{RRKM}}$ can be interpreted as the statistical unimolecular reaction rate corrected for the volume of trapped trajectories in the reactant phase space^{29,49,63,70}. The modified

statistical rate is therefore predicted to be *greater* than the RRKM rate, a prediction usually at odds with numerical simulations (cf. results presented below, also refs 47,49,63,70).

The low pressure ($\omega \rightarrow 0$) limit of the rate is

$$k_0(T) \equiv \lim_{\omega \rightarrow 0} k(T) = \frac{\omega}{Z_A} \int_{E_0}^{+\infty} dE e^{-\beta E} \int_{\text{DS}_{\text{in}}(E)} d\sigma s \quad (2.19a)$$

$$= \frac{\omega}{Z_A} \int_{E_0}^{+\infty} dE e^{-\beta E} \phi(E) \bar{s} \quad (2.19b)$$

$$= \frac{1}{Z_A} \int_{E_0}^{+\infty} dE \rho_A(E) e^{-\beta E} k_f^{\text{RRKM}}(E) \omega \bar{s} \quad (2.19c)$$

showing that the effective microcanonical rate is smaller than the RRKM statistical weight by a factor $\omega \bar{s} \ll 1$. That is, in the low pressure limit the reaction rate is proportional to the rate of collisional activation ω , with each molecule taking a time \bar{s} on average to react.

Different choices of transition state location will in general result in different mean gap times²⁹. We emphasize that exact and unambiguous calculation of the mean gap time (2.18) is possible given knowledge of the *phase space* geometrical structures that enable us to construct the reaction region, a dividing surface with minimal flux (hence the exact flux can be computed without integrating trajectories), and the reactive volume, i.e., the volume of the energy surface corresponding to interesting initial conditions $\mathbf{x} \in \mathcal{M}_A^C$. The fundamental geometrical structures required to compute these quantities are the $2n - 2$ dimensional hemispheres $\text{DS}_{\text{in}}(E)$ and $\text{DS}_{\text{out}}(E)$ that control the entrance to the reaction region and exit from the reaction region, respectively. These geometrical structures are what we use to compute flux and we sample initial conditions on $\text{DS}_{\text{in}}(E)$ and integrate them until they reach $\text{DS}_{\text{out}}(E)$ in order to compute $\bar{s}_{\text{DS}_{\text{in}}(E)}$. A detailed algorithm has previously been given for computing the dividing surfaces and the flux across them^{114,115,120}. In these references, numerical tests were also described for determining the range of energies above the saddle for which the dividing surface “locally disconnects” the energy surface in the way described above (in particular, for energies sufficiently larger than the saddle the dynamics may not “feel” the influence of the saddle point at all and the energy surface could deform so much that it would make no sense to speak of disjoint regions of “reactants” and “products”¹⁴⁹).

E. Multiple saddles

So far, we have only considered a reaction region where access in and out of the region is controlled by a single saddle. We can similarly consider a reaction region (in phase space) where access in and out of the region is controlled by d saddles (actually, d saddle-center-... - center type equilibria). Associated with each saddle we can compute a $2n - 2$ dimensional dividing surface, $DS_i(E)$, that is divided into two $2n - 2$ dimensional hemispheres $DS_{i,\text{in}}(E)$ and $DS_{i,\text{out}}(E)$ which have the same interpretation as above. The magnitude of the flux out of the reactive region is denoted by $\sum_{i=1}^d \phi_i(E)$ and it is shown in^{117,118} that the volume of initial conditions in the energy surface that correspond to trajectories that leave the reaction region is given by $\sum_{i=1}^d \bar{s}_{DS_{i,\text{in}}(E)} \phi_i(E)$, where $\bar{s}_{DS_{i,\text{in}}(E)}$ is the average time for trajectories starting on $DS_{i,\text{in}}(E)$ to cross $DS_{j,\text{out}}(E)$, for any $1 \leq j \leq d$. In this case the corrected total statistical escape rate is given by:

$$k_{f,C}^{\text{RRKM}}(E; d) = \frac{\sum_{i=1}^d \phi_i(E)}{\sum_{i=1}^d \bar{s}_{DS_{i,\text{in}}(E)} \phi_i(E)}. \quad (2.20)$$

An important case is that where all of the saddles are symmetric in the sense that $\phi_i(E) = \phi_j(E)$, $\bar{s}_{DS_{i,\text{in}}(E)} \phi_{i,\text{in}}(E) = \bar{s}_{DS_{j,\text{in}}(E)} \phi_{j,\text{in}}(E)$, for all $1 \leq i, j \leq d$ then the corrected statistical rate (2.20) reduces to expression (2.18).

The symmetric situation applies to the case of HCN isomerization considered in^{116,117}. Numerical results for HCN are further discussed in Sec. III of the present paper.

III. HCN ISOMERIZATION DYNAMICS

The isomerization dynamics of HCN, $\text{HCN} \rightleftharpoons \text{CNH}$, has been widely studied, using both classical and quantum mechanics: see, for example, refs 116,117,129,130,131,132,133,134, 135,136,137 and references therein. In the calculations reported in refs 116,117, the potential energy surface of Murrell, Carter, and Halonen (MCH)¹⁵⁰ was used. For the MCH potential energy surface the saddle point is at energy -12.08 eV and the trajectory calculations in refs 116,117 were all carried out at energy 0.2 eV above the saddle.

The HCN molecule is modelled as a planar system with zero angular momentum, so that there are three DoF^{116,117}. In planar HCN there are two saddles, related by reflection symmetry, separating reactant (HCN) from product (CNH), with bond angle $\gamma = \pm\gamma^* \simeq \pm 67^\circ$ (see Figure 2). The mean gap time is found to be $\bar{s} = 0.174$ ps which corresponds to an isomerization rate of 0.14×10^{-3} a.u.^{116,117} (see below). A discussion of numerical aspects and efficiency of the calculations was also given in refs 116,117.

A. Gap time and reactant lifetime distributions

The phase space structures of interest at fixed energy E , namely the NHIMs and the dividing surfaces separating reactant from product, are computed via an algorithmic procedure based on Poincaré-Birkhoff normalization that is described in refs 110,120. The Poincaré-Birkhoff normalization provides a nonlinear, symplectic transformation from the original, physical coordinates (q, p) to a new set of coordinates, the *normal form coordinates* (\bar{q}, \bar{p}) , in terms of which the dynamics is “simple”. Moreover, in these normal form coordinates the phase space structures governing reaction dynamics can be expressed in terms of explicit formulae, as described in refs 110,120. Their influence on the dynamics, in the normal form coordinates, is very easy to understand, and the geometrical structures can then be mapped back into the original coordinate system.

The Poincaré-Birkhoff normal form theory provides an algorithm to compute the symplectic transformation T from physical coordinate to normal coordinates,

$$T(q, p) = (\bar{q}, \bar{p}). \quad (3.1)$$

In a local neighbourhood \mathcal{L} of the equilibrium point of interest, this transformation “unfolds” the dynamics into a “reaction coordinate” and “bath modes”: expressing the system

Hamiltonian H in the new coordinates, (\bar{q}, \bar{p}) , via

$$H_{\text{NF}}(\bar{q}, \bar{p}) = H(T^{-1}(q, p)), \quad (3.2)$$

gives H_{NF} in a simplified form. This “unfolding” into a reaction coordinate and bath modes is one way of understanding how we are able to construct the phase space structures, in the normal form coordinates, that govern the dynamics of reaction. The explicit expressions for the coordinate transformations, $T(q, p) = (\bar{q}, \bar{p})$ and $T^{-1}(\bar{q}, \bar{p}) = (q, p)$, between the normal form (NF) coordinates and the original coordinates provided by the normalization procedure are also essential, as they allow us to transform the phase space structures constructed in normal form coordinates back into the original physical coordinates.

We consider an ensemble of trajectories with initial conditions sampled uniformly on one of the two dividing surfaces, $\text{DS}_{1,\text{in}}(E)$ say, according to the measure $d\sigma$ (cf. eq. (2.4)), so that all trajectories initially enter the reactant region of phase space via channel 1. Initial conditions on the dividing surface are obtained by uniformly sampling the $2n-2$ dimensional DS in normal form coordinates $(\bar{\mathbf{q}}, \bar{\mathbf{p}})$ with reaction coordinate variables (\bar{q}_1, \bar{p}_1) determined by energy conservation ($E = -11.88$ eV) together with the constraint $\bar{q}_1 = \bar{p}_1$. The inverse of the normal form coordinate transformation is used to compute physical coordinates for initial phase points, and trajectories are propagated forward in time in physical coordinates. As a trajectory approaches either dividing surface $\text{DS}_{i,\text{out}}(E)$, a transformation is made to normal form coordinates, which allows accurate determination of the time at which the trajectory crosses the out DS. This is the gap time.

The ensemble consists of 815871 trajectories; of these, 83599 ultimately exit through channel (DS) 1, while 732272 exit through channel 2. The branching ratio for the whole ensemble is then 8.76, very different from the statistical value unity dictated by symmetry. The mean gap time for the complete ensemble is 0.174 ps¹¹⁷. For trajectories reacting via channel 1, $\bar{s} = 0.714$ ps, while $\bar{s} = 0.112$ ps for those reacting via channel 2. Those trajectories that exit via the same transition state through which they entered therefore have a significantly larger average gap time. This makes physical sense, as such trajectories must have at least one turning point in the bending motion.

The gap time distribution $\mathcal{P}(s; E)$ for the complete ensemble at constant $E = -11.88$ eV is shown in Figure 3a (cf. Figure 4b of ref. 117). Gap time distributions for subensembles 1 and 2 are shown in Figures 3b and 3c, respectively. In addition to the gap time distribution

itself, we also consider the cumulative distribution $F(t)$, which is defined as the fraction of trajectories on the DS with gap times $s \geq t$, and is simply the product of the normalized reactant lifetime distribution function $\mathbb{P}(t; E)$ and the mean gap time \bar{s} (cf. eq. (2.12)):

$$F(t) = \int_t^{+\infty} ds \mathcal{P}(s; E) \quad (3.3a)$$

$$= \bar{s} \mathbb{P}(t; E). \quad (3.3b)$$

For the random gap time distribution (2.9), the cumulative gap time distribution is exponential, $F(t) = e^{-\mathbb{k}t}$.

Cumulative gap time distributions for $0 \leq t \leq 0.4$ ps are shown for the whole ensemble in Fig. 4a, and for the two subensembles in Figs 4b and 4c, respectively. Reactant lifetime distributions for the whole ensemble over longer time intervals ($0 \leq t \leq 25$ ps) are presented in Figure 5; both $\log[F(t)]$ vs t and $\log[F(t)]$ vs $\log t$ plots are shown. Corresponding plots for the two subensembles are shown in Figs 6 and 7.

We now discuss properties of the gap time and lifetime distributions on various physically relevant timescales:

1. Very short times ($t \ll \bar{s}$)

By construction, the phase space DS used to separate reactants and products eliminates local (short-time) recrossings^{109,110,114,115,116,117,118,119,120}. Hence, there are no very short gaps.

2. Short times ($t \simeq \bar{s}$).

The gap time distribution for the complete ensemble shows “pulses” of reacting trajectories. Each pulse is associated with a bundle of trajectories that execute a certain number of oscillations in the reactant well before crossing one or the other DS^{116,117}. The first pulse is associated with trajectories exiting via channel 2, the second pulse with trajectories exiting via channel 1, and so on. Similar structure has been seen in the lifetime distribution computed for escape of Rydberg electrons in crossed fields¹²⁷.

The cumulative gap time distributions up to times $\simeq \bar{s}$ (Fig. 4) exhibit a structured and faster-than-exponential decay and so cannot readily be fitted to an exponential curve in order to obtain an effective decay rate for trajectories leaving the HCN well.

3. Intermediate times $10\bar{s} \gtrsim t \gtrsim \bar{s}$.

On intermediate timescales, the peaks associated in the gap time distribution associated with individual pulses begin to overlap. The reactant lifetime distribution exhibits *algebraic* (power law) decay, $F(t) \sim 1/t^\alpha$, with $\alpha \simeq 0.705$ (Figure 5a). Such power law decay has been seen in other models for isomerization^{103,104}, and is in general associated with fractional kinetics¹⁰².

Attempts have been made to rationalize the existence of power law lifetime distributions in such systems in terms of a hierarchical set of bottlenecks, perhaps associated with the Arnold web^{51,93} presumed to exist in the vicinity of the minimum of the potential well. At this stage, however, a more quantitative explanation of the dynamical origins of algebraic decays such as those seen here at intermediate times remains an open problem.

On the same timescale, both subensembles exhibit algebraic decay with essentially *identical* exponents α : 0.708 and 0.701, respectively (Figs 6a, 7a). Of course, if one starts with an ensemble of reactant phase points whose distribution possesses the symmetry of the phase space induced by the reflection symmetry of the potential, then equality of the exponents for the algebraic portion of the decay is expected. Our ensemble of initial conditions is nevertheless highly asymmetric. We comment on the observed exponent equality further below in our discussion of branching ratios.

4. Long times $t \gg \bar{s}$.

At longer times the lifetime distribution exhibits exponential decay, $F(t) \sim e^{-kt}$, with exponent $k \simeq 0.092 \text{ ps}^{-1}$ (the decay constant is obtained by fitting the data for $10 \leq t \leq 20 \text{ ps}$, cf. Figure 5b). Decay constants k are found to be identical for trajectories exiting through either channel (0.093 ps^{-1} for channel 1, Fig 6b, 0.091 ps^{-1} for channel 2, Fig 7b). Again, equality of decay rates is expected on symmetry grounds for a symmetric ensemble. More generally, the equality of decay rates for trajectory subensembles reacting via distinct channels is an implicit assumption of statistical theories²⁹. An informative discussion of this equality is given in Sec. V(d) of ref. 29.

For a system such as HCN with 2 identical transition states the total forward decay

constant $k = k_f$.

B. Statistical and modified statistical rates

Having characterized the behavior of the gap time and lifetime distributions on various timescales, we now consider the relation of the numerically determined decay rate to various statistical estimates.

Figure 8 shows the survival probability $P_S(t)$ for phase points in the reactant region of phase space (cf. Fig. 3b of ref. 117). This quantity is computed by Monte Carlo sampling phase points \mathbf{x} in the reactant region, $\mathbf{x} \in \Sigma_E \cap \mathcal{M}_A$, and propagating trajectories until they either react through either channel or a cutoff time is reached. The fraction of phase points surviving until time t is $P_S(t)$. It can be seen that $P_S(t)$ appears to converge relatively slowly to a constant value $f_T = P_S(\infty) \simeq 0.91^{151}$. This shows that over 90% of phase points are trapped in the reactant region, and that the density of states $\rho_A^C = (1 - f_T)\rho_A$ associated with crossing trajectories is approximately 10% of the full reactant density of states ρ_A .

The value of ρ_A^C has also been computed using the relation

$$\rho_A^C = 2 \bar{s} \phi(E), \quad (3.4)$$

and shown to be identical with the result obtained via the survival probability¹¹⁷.

Numerical values of relevant quantities are $\bar{s} = 0.163$ ps, $\phi = 0.00085 \times h^2$, where h is Planck's constant, $\rho_A = 0.795 \times h^3/\text{eV}$ and $\rho_A^C = 0.0715 \times h^3/\text{eV}$. Computed values for the total statistical decay rate coefficient (in the symmetric case, equal to the single channel rate constant k_f) are $k_f^{\text{RRKM}} = 0.517 \text{ ps}^{-1}$ (RRKM, uncorrected) and $k_{f,C}^{\text{RRKM}} = 1/\bar{s} = 5.75 \text{ ps}^{-1}$ (RRKM, corrected). These values are to be compared with the long time decay rate $k = 0.092 \text{ ps}^{-1}$.

It is immediately apparent that, as noted previously (ref. 63, although cf. ref. 70), the value of the statistical rate constant “corrected” for the volume of trapped reactant phase points is both much larger than the uncorrected statistical rate and in significantly greater disagreement with the exact (numerical) value of k . In fact, the ratio $k_f^{\text{RRKM}}/k = 5.62$, so that the uncorrected statistical rate coefficient is within a factor of 6 of the numerical escape rate. This is presumably due to compensating errors in the statistical calculation⁶³. The presence of trapped regions of reactive phase space decreases the volume of phase space

that is available for reactive trajectories to explore; this effect tends to increase the value of the actual escape rate with respect to the statistical estimate. As can be seen from the numerical values given above, if this were the only factor affecting the rate then the actual rate would be a factor of 10 larger than the RRKM estimate. However, additional dynamical trapping mechanisms, that are as yet not fully understood for multimode systems^{85,93,152}, serve to delay the exit of phase points from the reactant region. The competition between these two effects then results in a value of the numerical escape rate that is fairly close to the simple RRKM estimate⁶³.

C. Statistical branching ratio accompanied by nonexponential decay

In Figure 9 we plot $\log[N(t)]$ versus t for each subsensemble, where $N(t)$ is the number of phase points remaining in the well at time t . Except at extremely short times $\lesssim 0.5$ ps, the two curves are essentially identical. For those times during which the decay curves are identical, the associated product branching ratio is equal to its statistical value, unity. The fact that the curves can be overlaid even at times for which the decay of each ensemble is nonexponential (algebraic) then implies that we have a statistical product ratio in the absence of exponential decay. (Note that exponential decay is usually taken to be the signature of “statistical” dynamics^{27,29}.) The identity of the decay curves also implies the equality of the algebraic decay exponents noted previously.

A qualitative explanation of this behavior is as follows: note that we start with a highly asymmetric initial ensemble, entering via $DS_{1,\text{in}}$ only. This bundle of trajectories passes through the HCN well, over to DS_2 . Some fraction of the ensemble exits through $DS_{2,\text{out}}$ and is lost. The rest of the trajectories then turn back, and pass through the well again, over to DS_1 . Some fraction is again lost. (These are the “pulses” seen in the short-time gap time distribution.) And so on.

The point is that, after the trajectory bundle has oscillated back and forth in the HCN well several times, the set of phase points still in the well behaves *as if* as if it were an ensemble consisting of trajectories initiated in equal numbers on both entry dividing surfaces and then propagated for $t \gtrsim 0.5$ ps. The underlying idea here is that, when trajectories are “turned back” from a DS, their subsequent time evolution can be qualitatively similar to that of trajectories actually initiated on the same DS. For example, trajectories turned back

at DS_2 that are just “outside” the incoming reactive cylinder manifold associated with the dividing surface^{72,110,120} will track (shadow¹⁵³) trajectories that actually enter the reactant region through $DS_{2,\text{in}}$ inside the reactive cylinder and lie close to the boundary (unstable manifold W^u).

The HCN gap time/lifetime distributions therefore imply that the initial ensemble effectively attains the full symmetry of the reactant phase space some time before it fully relaxes to the stage where exponential decay is observed²⁹, so that the system exhibits statistical branching ratios in the absence of exponential decay.

D. Comparison with other calculations

The trajectory calculations analyzed here were carried out using the MCH potential surface¹⁵⁰ at a constant energy $E = -11.88$ eV (0.2 eV above the saddle energy). Tang, Jang, Zhao and Rice (TJZR)¹³⁴ have carried out classical trajectory calculations using the same potential surface for a number of energies, and have applied an approximate version⁸² of the 3-state statistical theory of Gray and Rice⁷⁰ as well as a reaction path approach⁸³ to compute isomerization rate constants for the 3 DoF, zero angular momentum HCN isomerization.

The energy value used by TJZR closest to that of the present work is $E = -11.5$ eV. At this energy, TJZR extract an isomerization rate of 0.146×10^{-3} a.u. from their trajectory calculations, corresponding to a mean lifetime of 0.166 ps¹³⁴. This rate, which determines the timescale for decay of the CNH population and is therefore strictly the relaxation rate $k = k_f + k_b$ ^{60,61,70}, is actually obtained by computing the average escape time (lifetime) for an ensemble of trajectories in the CNH well, while somewhat arbitrarily omitting from consideration short-lived trajectories with lifetimes < 1500 a.u.¹³⁴.

The value of the mean lifetime computed by TJZR at $E = -11.5$ is close to the mean gap time (0.174 ps) computed at $E = -11.88$ eV¹¹⁷. Both approximate rate theories applied to the problem by TJZR give isomerization rates within factors of 2-3 of the trajectory values. These approximate statistical theories are however only capable of describing short time kinetics^{29,70}; the slow decays apparent from the trajectory data of TJZR (see Figure 7 of¹³⁴; cf. Figs 5, 6 and 7 of the present paper) are not predicted by 2- or 3-state statistical models. The algebraic decay observed at intermediate times in the present work suggests that incorporation of a small number of approximate intramolecular bottlenecks into the

statistical model^{67,69,70,82,84} is unlikely to lead to an accurate description of decay dynamics at longer times.

E. Relation to nonstatistical behavior in reactions of organic molecules

Finally, it is very interesting to note that the dynamical behavior associated with the gap time distribution analyzed here for HCN isomerization provides an exemplary instance of the highly nonstatistical dynamics discussed by Carpenter in the context of reactions of organic molecules^{46,47}.

Thus, as discussed above, an ensemble of trajectories is launched into a reactant region (the HCN well) for which there are two equivalent exits (“products”). Any statistical theory predicts a 1:1 branching ratio, as there is by symmetry equal probability of leaving via exit 1 or 2. The trajectory calculations however show that a significant fraction of the initial ensemble of trajectories simply passes through the HCN well and exits directly via channel 2 in a very short time; the remainder of the ensemble then sloshes back and forth in the well leading to the pulses seen at short times in the gap time distribution; these pulses are associated with bursts of exiting trajectories alternating between channels 2 and 1. At longer times, $t \gtrsim 0.5$ ps, we enter a regime in which decay into either channel is equally likely. By this time, however, most of the trajectories have already exited the well.

IV. SUMMARY AND CONCLUSION

In this paper we have revisited the general approach to classical unimolecular reaction rates due to Thiele²⁷ in light of recent advances in the phase space formulation of transition state theory for multidimensional systems^{105,109,110,114,115,116,117,118,119,120}. We showed that key concepts in Thiele’s approach, namely the phase space dividing surface separating reactants from products, the average gap time, and the volume of phase space associated with reactive (interesting⁹; crossing⁶³) trajectories, are both rigorously defined and readily computed within the phase space approach^{115,117,118,120}.

The distribution of gap times is a central element of Thiele’s approach^{27,29}. Here, we have analyzed in detail the gap time distribution and associated reactant lifetime distribution for the isomerization reaction $\text{HCN} \rightleftharpoons \text{CNH}$, previously studied using the methods of phase space transition state theory in refs 116,117. Both algebraic (power law) and exponential decay regimes have been identified. The dynamical origins of power law behavior or ‘fractional dynamics’ in multimode Hamiltonian systems, especially at intermediate times, remain obscure¹⁰². When combined with the normal form algorithm for computation and sampling of the phase space dividing surface, the cumulative gap time distribution is nevertheless a powerful diagnostic for reactive dynamics in multi-dimensional systems.

We have also compared statistical estimates of the isomerization rate^{27,29,63,114,117} with the numerically determined decay rate. We have found that, as noted by others⁶³, correcting the RRKM estimate to account for the measure of the reactant phase space region occupied by trapped trajectories results in a drastic overestimate of the isomerization rate. Compensating but as yet poorly understood trapping mechanisms in the reactant region serve to slow the escape rate sufficiently that the uncorrected RRKM estimate turns out to be reasonably accurate, at least at the particular energy studied.

In the planar model of HCN isomerization studied here, trajectories can exit the HCN well through either of 2 channels, where the channels are related by a reflection symmetry. Analysis of the decay properties of the subensembles of trajectories that exit through particular channels shows that, despite a highly asymmetric distribution of initial conditions, the complete trajectory ensemble effectively attains the full symmetry of the system phase space on a short timescale $t \lesssim 0.5$ ps, after which the product branching ratio is 1:1, the “statistical” value. However, at intermediate times, this statistical product ratio is accompanied

by *nonexponential* (algebraic) decay.

We have also pointed out the close parallels between the dynamical behavior inferred from the gap time distribution for HCN and nonstatistical dynamics in reactions of organic molecules discussed by Carpenter^{46,47}.

Acknowledgments

H.W. acknowledges EPSRC for support under grant number EP/E024629/1. S.W. acknowledges the support of the Office of Naval Research Grant No. N00014-01-1-0769.

APPENDIX A: DIVISION OF REACTANT PHASE SPACE INTO TRAPPED AND REACTIVE COMPONENTS

The Poincaré recurrence theorem^{143,154}, used in conjunction with the geometrical structures constructed in the phase space reaction rate theory described in Section II, allows us to give a precise treatment of the division of the reactant phase space into reactive (“crossing”) and trapped regions.

Suppose that, for a fixed energy E , there are d saddles associated with dividing surfaces $DS_i(E)$, $i = 1, \dots, d$, where each dividing surface is divided into two $2n - 2$ dimensional hemispheres $DS_{i,\text{in}}(E)$ and $DS_{i,\text{out}}(E)$ that control entrance and exit to a *compact* reactant region. We first show that every trajectory (except for a set of measure zero) that enters the reactant region through a dividing surface $DS_{i,\text{in}}(E)$ will exit the reactant region at a later time.

To this end, consider a set \bar{V} of (\bar{q}, \bar{p}) in $DS_{i,\text{in}}(E)$ of positive volume with respect to the (Lebesgue) measure $d\sigma = d^{n-1}\bar{q}d^{n-1}\bar{p}$. Suppose that the points in \bar{V} as a set of initial conditions for Hamilton’s equation give trajectories which stay in the reactants region for all time $\psi > 0$. Then the region swept out by these trajectories has infinite volume with respect to the (Lebesgue) measure $d\sigma \wedge d\psi$ (see Sec. II B). This contradicts the compactness of the reactant region. We can thus conclude that every initial condition on $DS_{i,\text{in}}(E)$ (except for a set of measure zero with respect to the measure $d\sigma = d^{n-1}\bar{q}d^{n-1}\bar{p}$) gives a trajectory which leaves the reactant region at a later time. This conclusion holds for both compact and noncompact (dissociative) product regions.

In the case that the product regions are also compact, we can invoke the Poincaré recurrence theorem for Hamiltonian dynamics on compact energy surfaces¹⁴³: *Consider any open set in a compact energy surface. Then, with the possible exception of a set of (Lebesgue) measure zero, trajectories of Hamilton’s equations with initial conditions starting in this open set return infinitely often to this set.*

Consider $DS_{i,\text{in}}(E)$, for any i . Trajectories starting on this surface must enter the reactant region. That is, the vector field defined by Hamilton’s equations, evaluated on $DS_{i,\text{in}}(E)$, is transverse to $DS_{i,\text{in}}(E)$ and pointing strictly into the reactant region (as proved in¹¹⁰). This is the mathematical manifestation of the “no-recrossing” property. Since the vector field defined by Hamilton’s equations points strictly into the reactant region on $DS_{i,\text{in}}(E)$ we can construct a “thin” open set, $\mathcal{O}_{i,\text{in}}(E)$, containing $DS_{i,\text{in}}(E)$ having the property that all trajectories starting in this open set also enter the region.

Now, by construction, no trajectory leaving $\mathcal{O}_{i,\text{in}}(E)$ and entering the reactant region can ever intersect $\mathcal{O}_{i,\text{in}}(E)$ *without* first leaving the region (which must occur through $DS_{j,\text{out}}(E)$, for some j). The reason for this is that the vector field defined by Hamilton’s equations restricted to $\mathcal{O}_{i,\text{in}}(E)$ is pointing strictly into the reactant region. By the Poincaré recurrence theorem, with the possible exception of a set of zero Lebesgue measure, every trajectory starting on $\mathcal{O}_{i,\text{in}}(E)$ intersects $\mathcal{O}_{i,\text{in}}(E)$ infinitely often. Therefore, we conclude that, with the possible exception of a set of zero Lebesgue measure, every trajectory that enters the reactant region exits and re-enters the region an infinite number of times. We can summarize as follows: *Almost all trajectories that enter a given reactant region of phase space exit the region at a later time. Moreover, after exiting, they will re-enter the same region at a later time, and this “entrance-exit” behaviour continues for all time thereafter.*

We can state this result also in a slightly different, but equivalent, way: *Almost all trajectories that exit given reactant region will return to the same region at a later time. Moreover, after returning, they will exit the region again at a later time, and this “exit-return” behaviour continues for all time thereafter.*

The immediate implication is that, with the possible exception of a set of Lebesgue measure zero, no trajectory can escape the reactant region of phase space that is *not* in the reactive (crossing) volume. The further implication is that, with the possible exception of a set of Lebesgue measure zero, the volume of the reactant region of phase space consists of two components— the reactive volume and the trapped volume. The boundary between

these two sets is liable to be exceedingly complicated (fractal¹⁵⁵).

APPENDIX B: DERIVATION OF THE DELAY DIFFERENTIAL EQUATION FOR $\mathbb{P}(t)$

In this Appendix we give a concise derivation of the delay differential equation satisfied by the reactant lifetime distribution $\mathbb{P}(t)$ in the DLGM of Dumont and Brumer²⁹. We consider a fixed value of the energy E .

In the notation of Sec. II C, the fraction of trajectories initiated on DS_{in} with gap time $s \geq t'$ is

$$\int_{t'}^{+\infty} ds \mathcal{P}(s) = \bar{s} \mathbb{P}(t'), \quad (\text{B1})$$

so that the probability of a trajectory initiated on DS_{in} having a gap time $t + t' \leq s \leq t + t' + dt$, $t \geq 0$, *given* that $s \geq t'$ is

$$\frac{\mathcal{P}(t + t')dt}{\bar{s} \mathbb{P}(t')} \quad (\text{B2})$$

The condition for statistical decay given by Dumont and Brumer can then be written²⁹

$$\frac{\mathcal{P}(t + t')}{\bar{s} \mathbb{P}(t')} = \mathbb{P}(t), \quad \forall t \geq 0, t' \geq \tau \quad (\text{B3})$$

where τ is the *relaxation time*. The meaning of this condition is as follows: consider those trajectories on DS_{in} with gap time $s \geq t'$; the fraction of these trajectories having gap times $t + t' \leq s \leq t + t' + dt$ is equal to $\mathbb{P}(t)dt$, the fraction of reactant phase points with lifetimes $t \rightarrow t + dt$, for $t' \geq \tau$. An equivalent formulation of the condition for statistical decay is

$$\frac{d}{dt} \mathbb{P}(t + t') = -\mathbb{P}(t)\mathbb{P}(t') \quad \forall t \geq 0, t' \geq \tau. \quad (\text{B4})$$

Conditions (B3) and (B4) are clearly satisfied in the case of an exponential lifetime distribution, $\mathbb{P}(t) = \mathbb{k}e^{-\mathbb{k}t}$.

To obtain the Delayed Lifetime Gap Model²⁹ for the lifetime distribution:

- Consider the gap time distribution $\mathcal{P}(t)$ for the *statistical* component of reactive phase space *only*. The reactive phase space has to be partitioned into a direct and a statistical component, perhaps using a trajectory divergence criterion²⁹.

- Set $k_S \equiv (\bar{s})^{-1}$, where the mean gap time is evaluated by averaging over the statistical component only. We therefore have $\mathbb{P}(0) = k_S$
- Assume that there are no gaps in the statistical component for $s < \tau$. That is, $\mathcal{P}(s) = 0$ for $s < \tau$ which implies $\mathbb{P}(t) = k_S$, $0 \leq t \leq \tau$.
- Set $t' = \tau$ (the relaxation time) to obtain the delay differential equation for the DLGM lifetime distribution:

$$\frac{d}{dt} \mathbb{P}(t + \tau) = -k_S \mathbb{P}(t) \quad \forall t \geq 0 \quad (\text{B5})$$

This equation can be solved using the Laplace-Fourier transform²⁹.

* gsel@cornell.edu

† H.Waalkens@rug.nl

‡ stephen.wiggins@mac.com

¹ R. Marcelin, *Annales de Physique* **3**, 120 (1915).

² O. K. Rice and H. C. Ramsperger, *J. Am. Chem. Soc.* **49**, 1617 (1927).

³ L. S. Kassel, *J. Phys. Chem.* **32**, 225 (1928).

⁴ L. S. Kassel, *J. Phys. Chem.* **32**, 1065 (1928).

⁵ R. A. Marcus and O. K. Rice, *J. Phys. Colloid Chem.* **55**, 894 (1951).

⁶ R. A. Marcus, *J. Chem. Phys.* **20**, 359 (1952).

⁷ L. S. Kassel, *The Kinetics of Homogenous Gas Reactions* (Chemical Catalog Company, New York, 1932).

⁸ C. N. Hinshelwood, *The Kinetics of Chemical Change* (Clarendon Press, Oxford, 1940).

⁹ N. B. Slater, *Theory of Unimolecular Reactions* (Cornell University Press, Ithaca, NY, 1959).

¹⁰ D. L. Bunker, *Theory of Elementary Gas Reaction Rates* (Pergamon, Oxford, 1966).

¹¹ H. S. Johnston, *Gas Phase Reaction Rate Theory* (Ronald Press, New York, 1966).

¹² O. K. Rice, *Statistical Mechanics, Thermodynamics, and Kinetics* (W. H. Freeman, San Francisco, 1967).

¹³ K. J. Laidler, *Theories of Chemical Reaction Rates* (McGraw-Hill, New York, 1969).

¹⁴ P. J. Robinson and K. A. Holbrook, *Unimolecular Reactions* (Wiley, New York, 1972).

- ¹⁵ W. Forst, *Theory of Unimolecular Reactions* (Academic, New York, 1973).
- ¹⁶ E. E. Nikitin, *Theory of Elementary Atomic and Molecular Processes* (Clarendon Press, Oxford, 1974).
- ¹⁷ I. W. M. Smith, *Kinetics and Dynamics of Elementary Gas Reactions* (Butterworths, London, 1980).
- ¹⁸ J. H. Beynon and J. R. Gilbert, *Application of Transition State Theory to Unimolecular Reactions: an Introduction* (Wiley, New York, 1984).
- ¹⁹ H. O. Pritchard, *The Quantum Theory of Unimolecular Reactions* (Cambridge University Press, Cambridge, 1984).
- ²⁰ D. Wardlaw and R. A. Marcus, *Adv. Chem. Phys.* **70**, 231 (1988).
- ²¹ R. G. Gilbert and S. C. Smith, *Theory of Unimolecular and Recombination Reactions* (Blackwell Scientific, Oxford, 1990).
- ²² T. Baer and W. L. Hase, *Unimolecular Reaction Dynamics* (Oxford University Press, New York, 1996).
- ²³ W. Forst, *Unimolecular Reactions* (Cambridge University Press, Cambridge, 2003).
- ²⁴ N. E. Henriksen and F. Y. Hansen, *Theories of Molecular Reaction Dynamics: The Microscopic Foundation of Chemical Kinetics* (Oxford University Press, New York, 2008).
- ²⁵ E. Pollak and P. Talkner, *CHAOS* **15**, 026116 (2005).
- ²⁶ N. B. Slater, *J. Chem. Phys.* **24**(6), 1256 (1956).
- ²⁷ E. Thiele, *J. Chem. Phys.* **36**(6), 1466 (1962).
- ²⁸ D. Bunker and W. L. Hase, *J. Chem. Phys.* **59**, 4621 (1973).
- ²⁹ R. S. Dumont and P. Brumer, *J. Phys. Chem.* **90**, 3509 (1986).
- ³⁰ R. S. Dumont and P. Brumer, *Chem. Phys. Lett.* **188**, 565 (1992).
- ³¹ R. S. Dumont, *J. Chem. Phys.* **91**, 4679 (1989).
- ³² R. S. Dumont, *J. Chem. Phys.* **91**, 6839 (1989).
- ³³ R. S. Dumont and S. Jain, *J. Chem. Phys.* **97**, 1227 (1992).
- ³⁴ S. Jain, S. Bleher, and R. S. Dumont, *J. Chem. Phys.* **99**, 7793 (1993).
- ³⁵ P. Brumer, D. E. Fitz, and D. Wardlaw, *J. Chem. Phys.* **72**(1), 386 (1980).
- ³⁶ E. Pollak, *J. Chem. Phys.* **74**, 6763 (1981).
- ³⁷ M. Tabor, *Adv. Chem. Phys.* **XLVI**, 73 (1981).
- ³⁸ S. A. Rice, *Adv. Chem. Phys.* **XLVII**, 117 (1981).

- ³⁹ P. Brumer, Adv. Chem. Phys. **XLVII**, 201 (1981).
- ⁴⁰ P. Brumer and M. Shapiro, Adv. Chem. Phys. **70**, 365 (1988).
- ⁴¹ S. Nordholm and S. A. Rice, J. Chem. Phys. **62**, 157 (1975).
- ⁴² S. A. Rice, J. Stat. Phys. **101**, 187 (2000).
- ⁴³ J. B. Gong and P. Brumer, Ann. Rev. Phys. Chem. **56**, 1 (2005).
- ⁴⁴ E. Thiele, M. F. Goodman, and J. Stone, Opt. Eng. **19**(6), 10 (1980).
- ⁴⁵ B. K. Carpenter, Acc. Chem. Res. **25**, 520 (1992).
- ⁴⁶ B. K. Carpenter, J. Phys. Org. Chem. **16**, 858 (2003).
- ⁴⁷ B. K. Carpenter, Ann. Rev. Phys. Chem. **56**, 57 (2005).
- ⁴⁸ A. Bach, J. M. Hostettler, and P. Chen, J. Chem. Phys. **125**, Art. No. 024304 (2006).
- ⁴⁹ M. Berblinger and C. Schlier, J. Chem. Phys. **101**, 4750 (1994).
- ⁵⁰ R. S. MacKay and J. D. Meiss, *Hamiltonian Dynamical Systems: A reprint selection* (Taylor and Francis, London, 1987).
- ⁵¹ A. J. Lichtenberg and M. A. Lieberman, *Regular and Chaotic Dynamics* (Springer Verlag, New York, 1992), 2nd ed.
- ⁵² S. Wiggins, *Chaotic transport in dynamical systems* (Springer-Verlag, 1992).
- ⁵³ V. I. Arnold, V. V. Kozlov, and A. I. Neishtadt, *Mathematical Aspects of Classical and Celestial Mechanics* (Springer, New York, 2006).
- ⁵⁴ P. Pechukas, Ann. Rev. Phys. Chem. **32**, 159 (1981).
- ⁵⁵ P. Pechukas, Ber. Buns. Ges. **86**, 372 (1982).
- ⁵⁶ E. Pollak, *Periodic orbits and the theory of reactive scattering* (CRC Press, Boca Raton, 1985), vol. 3 of *Theory of Chemical Reaction Dynamics*, pp. 123–246.
- ⁵⁷ E. P. Wigner, Trans. Faraday Soc. **34**, 29 (1938).
- ⁵⁸ D. G. Truhlar, B. C. Garrett, and S. J. Klippenstein, J. Phys. Chem. **100**, 12711 (1996).
- ⁵⁹ C. Jaffe, D. Farrelly, and T. Uzer, Phys. Rev. Lett. **84**, 610 (2000).
- ⁶⁰ D. Chandler, J. Chem. Phys. **68**, 2959 (1978).
- ⁶¹ D. Chandler, *Introduction to Modern Statistical Mechanics* (Oxford University Press, New York, 1987).
- ⁶² N. DeLeon and B. J. Berne, J. Chem. Phys. **75**, 3495 (1981).
- ⁶³ B. J. Berne, N. DeLeon, and R. O. Rosenberg, J. Phys. Chem. **86**, 2166 (1982).
- ⁶⁴ M. J. Davis and R. T. Skodje, *Chemical Reactions as Problems in Nonlinear Dynamics* (JAI

- Press, Greenwich, CT, 1992), vol. 3 of *Advances in Classical Trajectory Methods*, pp. 77–164.
- ⁶⁵ D. Bensimon and L. Kadanoff, *Physica D* **13**, 82 (1984).
 - ⁶⁶ R. S. MacKay, J. D. Meiss, and I. C. Percival, *Physica D* **13**, 55 (1984).
 - ⁶⁷ M. J. Davis, *J. Chem. Phys.* **83**, 1016 (1985).
 - ⁶⁸ S. R. Channon and J. L. Lebowitz, *Ann. NY Acad. Sci.* **357**, 108 (1980).
 - ⁶⁹ S. K. Gray and M. J. Davis, *J. Chem. Phys.* **84**, 5389 (1986).
 - ⁷⁰ S. K. Gray and S. A. Rice, *J. Chem. Phys.* **86**, 2020 (1987).
 - ⁷¹ C. C. Marston and N. DeLeon, *J. Chem. Phys.* **91**, 3392 (1989).
 - ⁷² A. M. O. DeAlmeida, N. DeLeon, M. A. Mehta, and C. C. Marston, *Physica D* **46**, 265 (1990).
 - ⁷³ N. DeLeon, M. A. Mehta, and R. Q. Topper, *J. Chem. Phys.* **94**, 8310 (1991).
 - ⁷⁴ N. DeLeon, M. A. Mehta, and R. Q. Topper, *J. Chem. Phys.* **94**, 8329 (1991).
 - ⁷⁵ N. DeLeon, *Chem. Phys. Lett.* **189**, 371 (1992).
 - ⁷⁶ N. DeLeon, *J. Chem. Phys.* **96**, 285 (1992).
 - ⁷⁷ N. DeLeon and S. Ling, *J. Chem. Phys.* **101**, 4790 (1994).
 - ⁷⁸ S. H. Tersigni and S. A. Rice, *Berichte der Bunsen-Gesellschaft (Phys. Chem. Chem. Phys.)* **92**, 227 (1988).
 - ⁷⁹ S. H. Tersigni, P. Gaspard, and S. A. Rice, *J. Chem. Phys.* **92**, 1775 (1990).
 - ⁸⁰ S. K. Gray, S. A. Rice, and M. J. Davis, *J. Phys. Chem.* **90**, 3470 (1986).
 - ⁸¹ M. Zhao and S. A. Rice, *J. Chem. Phys.* **96**, 3542 (1992).
 - ⁸² M. Zhao and S. A. Rice, *J. Chem. Phys.* **96**, 6654 (1992).
 - ⁸³ S. M. Jang and S. A. Rice, *J. Chem. Phys.* **99**, 9585 (1993).
 - ⁸⁴ S. A. Rice and M. S. Zhao, *Int. J. Quantum Chem.* **58**, 593 (1996).
 - ⁸⁵ M. Toda, *Adv. Chem. Phys.* **123**, 153 (2002).
 - ⁸⁶ V. I. Arnold, *Soviet Math. Doklady* **5**, 581 (1964).
 - ⁸⁷ P. Lochak, in *Hamiltonian Systems with Three or More Degrees of Freedom*, edited by C. Simo (Kluwer, Dordrecht, 1999), pp. 168–183.
 - ⁸⁸ E. J. Heller, *J. Phys. Chem.* **99**, 2625 (1995).
 - ⁸⁹ E. J. Heller, *J. Phys. Chem. A* **103**, 10433 (1999).
 - ⁹⁰ D. M. Leitner and P. G. Wolynes, *Phys. Rev. Lett.* **79**, 55 (1997).
 - ⁹¹ S. Keshavamurthy, *Int. Rev. Phys. Chem.* **26**, 521 (2007).
 - ⁹² M. Toda, *Adv. Chem. Phys.* **130 A**, 337 (2005).

- ⁹³ A. Shojiguchi, C. B. Li, T. Komatsuzaki, and M. Toda, Comm. Nonlinear Sci. Numerical Simulation **13**, 857 (2008).
- ⁹⁴ S. A. Schofield and P. G. Wolynes, Chem. Phys. Lett. **217**, 497 (1994).
- ⁹⁵ M. Gruebele, Adv. Chem. Phys. **114**, 193 (2000).
- ⁹⁶ M. Gruebele and P. G. Wolynes, Acc. Chem. Res. **37**, 261 (2004).
- ⁹⁷ D. M. Leitner and P. G. Wolynes, Chem. Phys. **329**, 163 (2006).
- ⁹⁸ D. M. Leitner and M. Gruebele, Mol. Phys. **106**, 433 (2008).
- ⁹⁹ S. A. Schofield and P. G. Wolynes, J. Chem. Phys. **98**, 1123 (1993).
- ¹⁰⁰ S. A. Schofield, P. G. Wolynes, and R. E. Wyatt, Phys. Rev. Lett. **74**, 3720 (1995).
- ¹⁰¹ S. Keshavamurthy, Chem. Phys. Lett. **300**, 281 (1999).
- ¹⁰² G. Zaslavsky, *Hamiltonian Chaos and Fractional Dynamics* (Oxford University Press, New York, 2005).
- ¹⁰³ A. Shojiguchi, C. B. Li, T. Komatsuzaki, and M. Toda, Phys. Rev. E **75**, 035204 (2007).
- ¹⁰⁴ A. Shojiguchi, C. B. Li, T. Komatsuzaki, and M. Toda, Phys. Rev. E **76**, 056205 (2007).
- ¹⁰⁵ S. Wiggins, Physica D **44**, 471 (1990).
- ¹⁰⁶ S. Wiggins, *Normally hyperbolic invariant manifolds in dynamical systems* (Springer-Verlag, 1994).
- ¹⁰⁷ E. Pollak and P. Pechukas, J. Chem. Phys. **69**, 1218 (1978).
- ¹⁰⁸ The co-dimension of a submanifold is the dimension of the space in which the submanifold exists, minus the dimension of the submanifold. The significance of a submanifold being “co-dimension one” is that it is one less dimension than the space in which it exists. Therefore it can “divide” the space and act as a separatrix, or barrier, to transport.
- ¹⁰⁹ S. Wiggins, L. Wiesenfeld, C. Jaffe, and T. Uzer, Phys. Rev. Lett. **86**(24), 5478 (2001).
- ¹¹⁰ T. Uzer, C. Jaffe, J. Palacian, P. Yanguas, and S. Wiggins, Nonlinearity **15**, 957 (2002).
- ¹¹¹ R. E. Gillilan, J. Chem. Phys. **93**, 5300 (1990).
- ¹¹² R. E. Gillilan and G. S. Ezra, J. Chem. Phys. **94**, 2648 (1991).
- ¹¹³ M. Toda, Phys. Rev. Lett. **74**, 2670 (1995).
- ¹¹⁴ H. Waalkens, A. Burbanks, and S. Wiggins, J. Phys. A **37**, L257 (2004).
- ¹¹⁵ H. Waalkens and S. Wiggins, J. Phys. A **37**, L435 (2004).
- ¹¹⁶ H. Waalkens, A. Burbanks, and S. Wiggins, J. Chem. Phys. **121**(13), 6207 (2004).
- ¹¹⁷ H. Waalkens, A. Burbanks, and S. Wiggins, Physical Review Letters **95**, 084301 (2005).

- 118 H. Waalkens, A. Burbanks, and S. Wiggins, J. Phys. A **38**, L759 (2005).
- 119 R. Schubert, H. Waalkens, and S. Wiggins, Phys. Rev. Lett. **96**, 218302 (2006).
- 120 H. Waalkens, R. Schubert, and S. Wiggins, Nonlinearity **21**(1), R1 (2008).
- 121 T. Komatsuzaki and R. S. Berry, J. Mol. Struct. THEOCHEM **506**, 55 (2000).
- 122 T. Komatsuzaki and R. S. Berry, Adv. Chem. Phys. **123**, 79 (2002).
- 123 T. Komatsuzaki, K. Hoshino, and Y. Matsunaga, Adv. Chem. Phys. **130 B**, 257 (2005).
- 124 L. Wiesenfeld, A. Faure, and T. Johann, J. Phys. B **36**, 1319 (2003).
- 125 L. Wiesenfeld, J. Phys. A **37**, L143 (2004).
- 126 L. Wiesenfeld, Few Body Syst. **34**, 163 (2004).
- 127 F. Gabern, W. S. Koon, J. E. Marsden, and S. D. Ross, Physica D **211**, 391 (2005).
- 128 F. Gabern, W. S. Koon, J. E. Marsden, and S. D. Ross, Few-Body Systems **38**, 167 (2006).
- 129 S. K. Gray, W. H. Miller, Y. Yamaguchi, and H. F. Schaefer, J. Chem. Phys. **73**, 2733 (1980).
- 130 M. Perić and M. Mladenović and S. D. Peyerimhoff and R. J. Buenker, Chem. Phys. **82**, 317 (1983).
- 131 M. Perić and M. Mladenović and S. D. Peyerimhoff and R. J. Buenker, Chem. Phys. **86**, 85 (1984).
- 132 B. L. Lan and J. M. Bowman, J. Phys. Chem. **97**, 12535 (1993).
- 133 J. A. Bentley, C. M. Huang, and R. E. Wyatt, J. Chem. Phys. **98**, 5207 (1993).
- 134 H. Tang, S. Jang, M. Zhao, and S. A. Rice, J. Chem. Phys. **101**(10), 8737 (1994).
- 135 S. P. Shah and S. A. Rice, Faraday Disc. **113**, 319 (1999).
- 136 C. B. Li, Y. Matsunaga, M. Toda, and T. Komatsuzaki, J. Chem. Phys. **123**, Art. No. 184301 (2005).
- 137 J. B. Gong, A. Ma, and S. A. Rice, J. Chem. Phys. **122**, 144311 (2005).
- 138 E. P. Wigner, J. Chem. Phys. **7**, 646 (1939).
- 139 J. C. Keck, Adv. Chem. Phys. **XIII**, 85 (1967).
- 140 J. B. Anderson, Adv. Chem. Phys. **XCI**, 381 (1995).
- 141 D. J. Wales, *Energy Landscapes* (Cambridge University Press, Cambridge, 2003).
- 142 Such a separation is assumed to be meaningful for the range of energies considered here.
- 143 V. I. Arnold, *Mathematical Methods of Classical Mechanics*, vol. 60 of *Graduate Texts in Mathematics* (Springer, New York, Heidelberg, Berlin, 1978).
- 144 J. Binney, O. E. Gerhard, and P. Hut, Mon. Not. Roy. Astron. Soc. **215**, 59 (1985).

- ¹⁴⁵ H.-D. Meyer, J. Chem. Phys. **84**, 3147 (1986).
- ¹⁴⁶ M. Toller, G. Jacucci, G. DeLorenzi, and C. P. Flynn, Phys. Rev. B **32**, 2082 (1985).
- ¹⁴⁷ R. S. MacKay, Phys. Lett. A **145**, 425 (1990).
- ¹⁴⁸ J. N. Stember and G. S. Ezra, Chem. Phys. **337**, 11 (2007).
- ¹⁴⁹ C. B. Li, A. Shojiguchi, M. Toda, and T. Komatsuzaki, Phys. Rev. Lett. **97**, Art. No. 028302 (2006).
- ¹⁵⁰ J. N. Murrell, S. Carter, and L. O. Halonen, J. Mol. Spect. **93**, 307 (1982).
- ¹⁵¹ The quantity f_T is therefore the effective value for the fraction of trapped states as determined on the timescale of the calculation. The true behavior of the survival probability $P_S(t)$ at *extremely* long times has not however been fully characterized, and merits further study.
- ¹⁵² R. Paskauskas, C. Chandre, and T. Uzer, Phys. Rev. Lett. **100**, 083001 (2008).
- ¹⁵³ J. Guckenheimer and P. Holmes, *Nonlinear Oscillations, Dynamical Systems, and Bifurcations of Vector Fields* (Springer, New York, 1983).
- ¹⁵⁴ G. D. Birkhoff, Bull. Am. Math. Soc. **38**, 361 (1931).
- ¹⁵⁵ E. Ott, *Chaos in Dynamical Systems* (Cambridge University Press, Cambridge, 2002), 2nd ed.

FIGURE CAPTIONS

FIG. 1: Phase space structures for unimolecular reaction (schematic). (a) Definition of reactant region, NHIM and dividing surface $DS(E) = DS_{\text{in}}(E) \cup DS_{\text{out}}(E)$. (b) Definition of gap time s and lifetime t .

FIG. 2: Isopotential surfaces of the HCN potential energy surface of ref. 150 in polar representation of the Jacobi coordinates r , R , and γ .

FIG. 3: HCN gap time distribution $\mathcal{P}(s)$. (a) Complete ensemble. (b) Subensemble reacting via channel 1. (c) Subensemble reacting via channel 2.

FIG. 4: HCN cumulative gap time (reactant lifetime) distribution $F(t)$ at short times. $\text{Log}F(t)$ is plotted vs t for $0 \leq t \leq 0.4$ ps. (a) Total ensemble. (b) Subensemble reacting via channel 1. (c) Subensemble reacting via channel 2.

FIG. 5: Cumulative gap time (reactant lifetime) distribution $F(t)$ for the complete ensemble. (a) A log-log plot shows power law decay at intermediate times. (b) Log plot shows exponential decay ($10 \leq t \leq 20$ ps).

FIG. 6: Cumulative gap time (reactant lifetime) distribution $F(t)$ for the subensemble reacting via channel 1. (a) A log-log plot shows power law decay at intermediate times. (b) Log plot shows exponential decay ($10 \leq t \leq 20$ ps).

FIG. 7: Cumulative gap time (reactant lifetime) distribution $F(t)$ for the subensemble reacting via channel 2. (a) A log-log plot shows power law decay at intermediate times. (b) Log plot shows exponential decay ($10 \leq t \leq 20$ ps).

FIG. 8: HCN survival probability $P_S(t)$. $P_S(t)$ is the fraction of an ensemble of trajectories uniformly distributed throughout the HCN region of phase space at $t = 0$ remaining in the well at time t . Trajectories are removed from the ensemble once they exit the HCN region by crossing $DS_{j,\text{out}}$, $j = 1, 2$; they cannot re-enter the region.

FIG. 9: The log of the number $N(t)$ of trajectories remaining at time t versus t is plotted for each subensemble: channel 1 (blue), channel 2 (red).

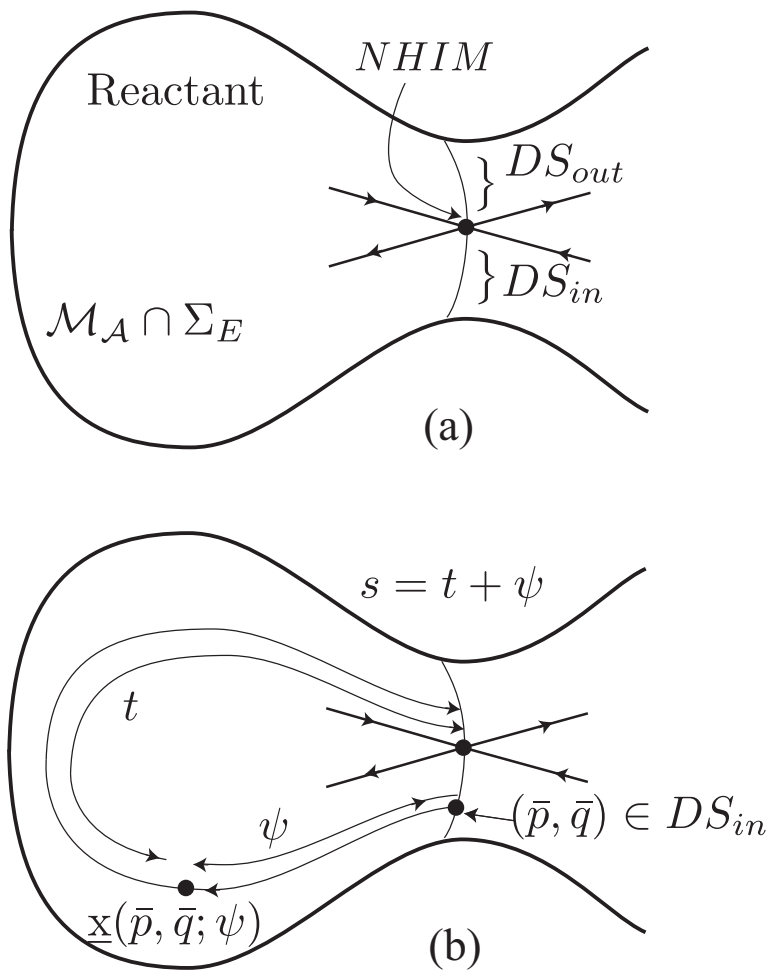


FIGURE 1

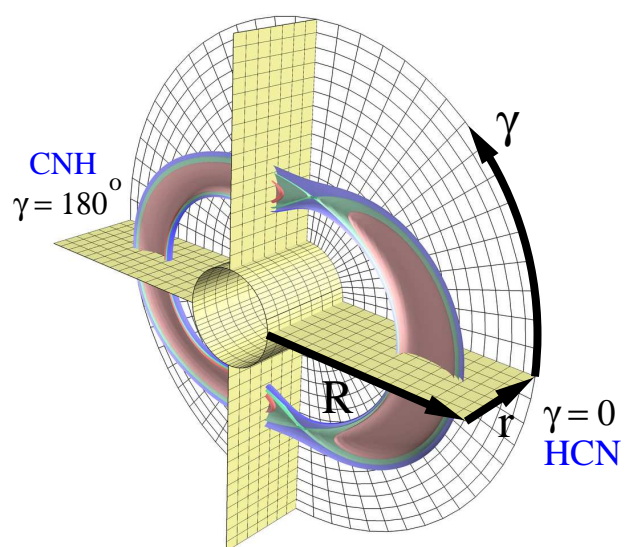


FIGURE 2

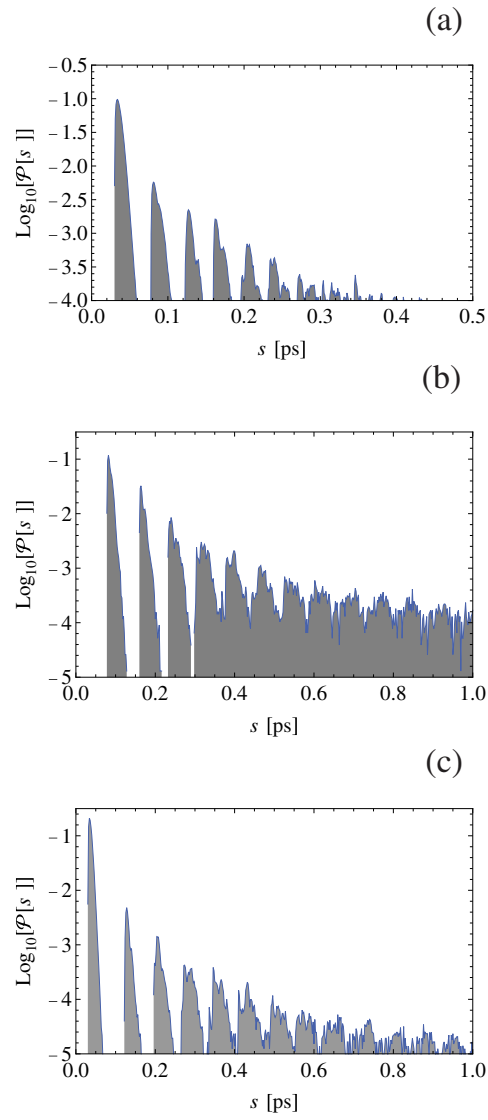


FIGURE 3

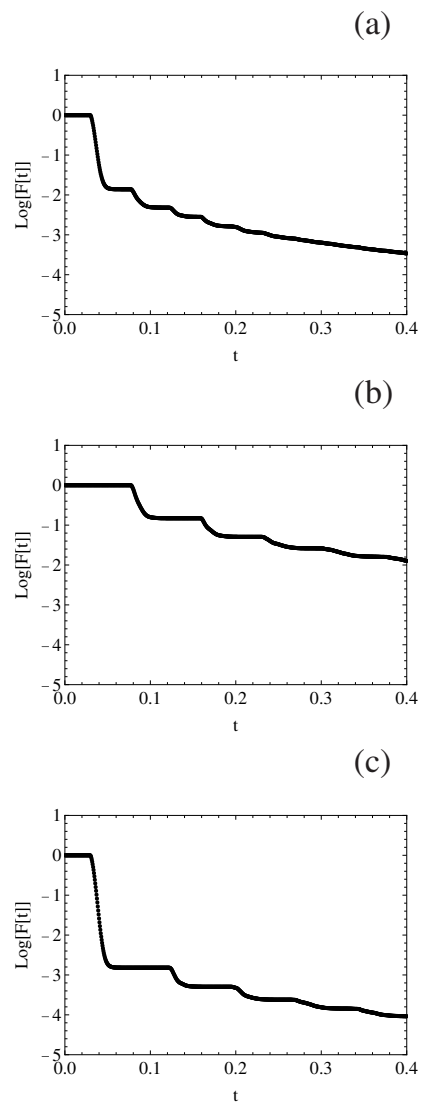


FIGURE 4

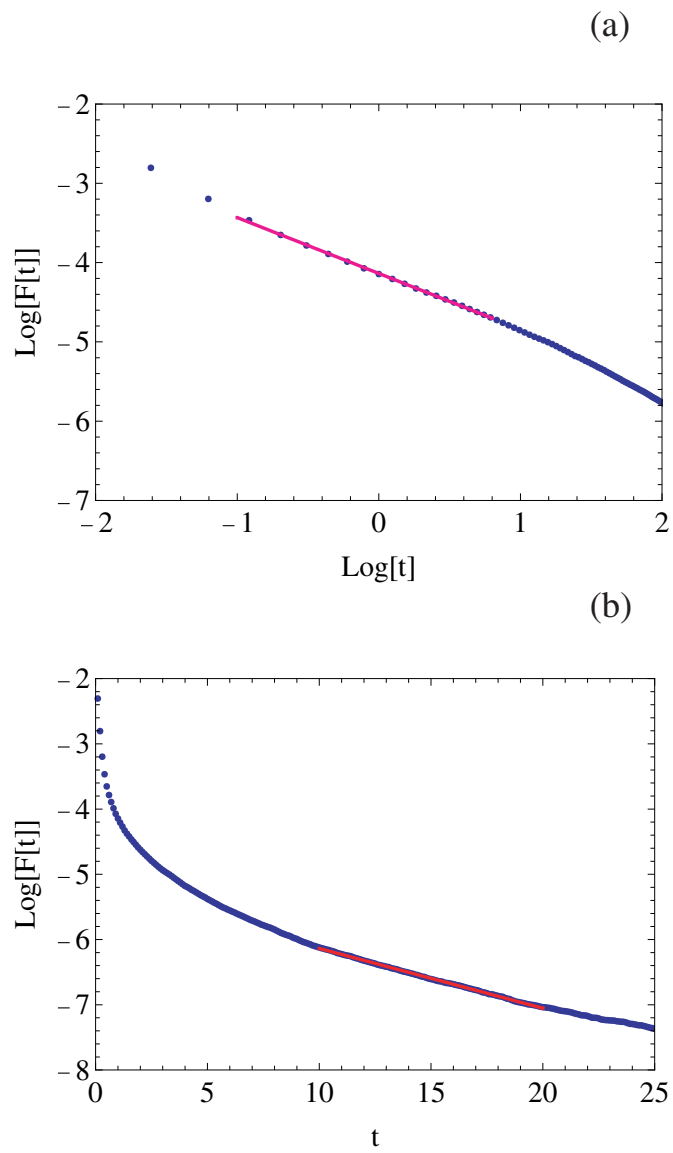


FIGURE 5

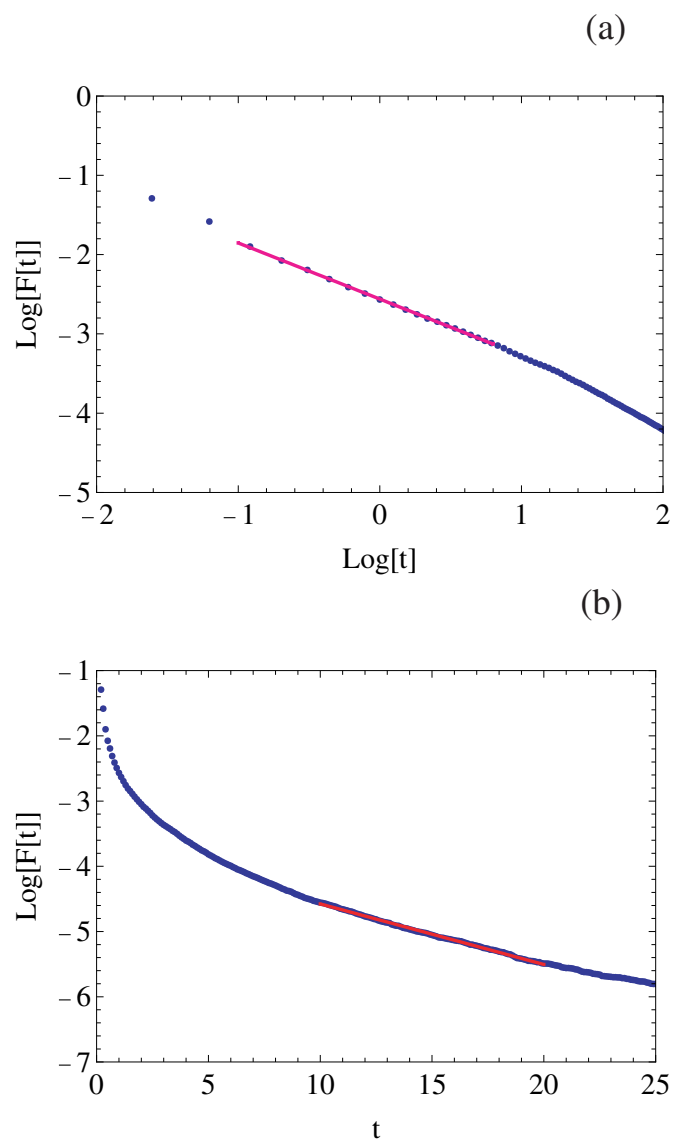


FIGURE 6

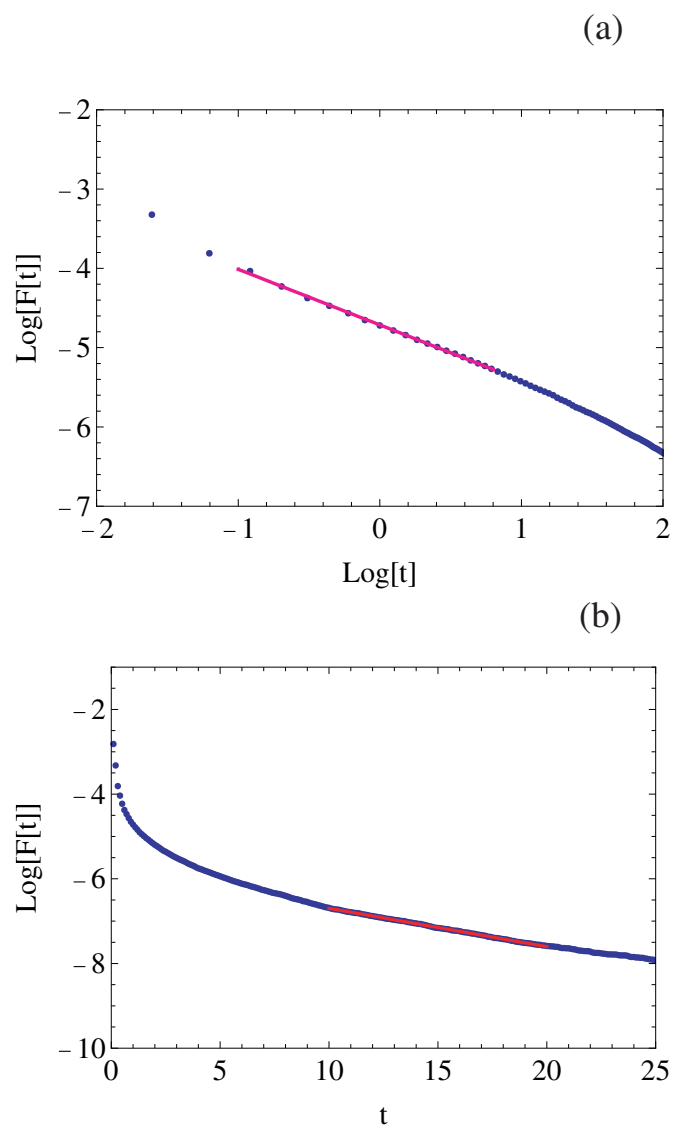


FIGURE 7

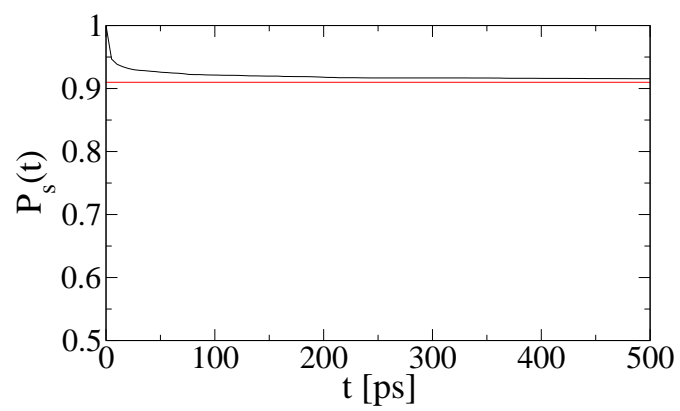


FIGURE 8

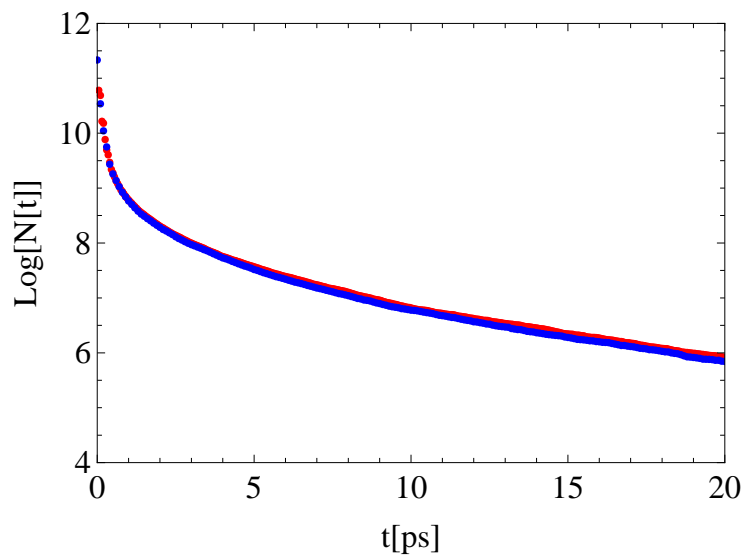


FIGURE 9